NONINTERCEPTING EMITTANCE MONITOR*

R. H. MILLER, J. E. CLENDENIN, M. B. JAMES, J. C. SHEPPARD
Stanford Linear Accelerator Center
Stanford University, Stanford, California 94305

Abstract A nonintercepting emittance monitor is a helpful device for measuring and improving particle beams in accelerators and storage rings as it allows continuous monitoring of the beam's distribution in phase space, and perhaps closed loop computer control of the distributions. Stripline position monitors are being investigated for use as nonintercepting emittance monitors for a beam focused by a FODO array in the first 100 meters of our linear accelerator. The technique described here uses the signal from the four stripline probes of a single position monitor to measure the quadrupole mode of the wall current in the beam pipe. This current is a function of the quadrupole moment of the beam, $\sigma_x^2 - \sigma_y^2$. In general, six independent measurements of the quadrupole moment are necessary to determine the beam emittance. This technique is dependent on the characteristically large variations of $\sigma_x^2 - \sigma_y^2$ in a FODO array. It will not work in a focusing system where the beam is round at each focusing element.

Introduction The Stanford Linear Collider (SLC) calls for very high current ($\sim$1 kA peak), very short pulse ($\sim$ 10 psec) electron beam, with a transverse emittance area no greater than $3 \times 10^{-3}\pi$ m_0c-cm. To achieve this emittance specification, the electron beam is accelerated to 1 GeV and then injected into a damping ring where its transverse emittance is reduced by a factor of 10. In order to successfully transmit the beam from the injector to the damping ring, the beam emittance must be known. Before the present study was undertaken, it was not possible to measure emittance without interrupting beam operation. The measurement technique described below makes possible continuous monitoring of beam emittance, and appropriate adjustment of the FODO lattice.

The beam emittance can be measured by sampling the image currents produced by a charged particle beam moving through a conducting pipe. These image currents can be expressed as a multipole expansion of the ratio of beam radius to pipe radius, r/a. The quadradic term in the expansion is a function of the beam's quadrupole moment, $\sigma_x^2 - \sigma_y^2$.

A number of devices can be used to measure the quadrupole moment including (1) the strip line position monitors discussed in this paper, (2) a cylindrical microwave cavity resonant in the $TM_{2,1,0}$ mode at the rf frequency of the beam, (3) a resisitively loaded insulated gap in the beam pipe with voltage monitors at four points around the gap, and (4) four magnetic pickup loops located at 90^o intervals around the beam pipe. All of these devices depend on the beam having a short time structure. Each device measures the $\cos 2\theta$ component of the image currents. For a long beam pulse with rf structure, the $TM_{2,1,0}$ microwave cavity is probably the most sensitive transducer, while for the very short pulses required for the SLC the stripline position monitors are ideal.

As part of the linac upgrade for the SLC, traveling wave stripline monitors have been installed in each of the quadrupole magnets spaced 12 meters apart along the linac. The monitors are currently used to measure the beam's intensity and transverse position. These monitors consist of four strips, each 13 cm long, grounded at their downstream ends (see Fig. 1). The beam induced pulse is read out at the upstream end of each strip and for an electron beam has a leading negative pulse followed $2\ell/c$ sec later by a positive pulse.[1,2] The pulses are stretched, combined into a single pulse with a DC restorer, and digitized. The signal on each strip is a function of the multipole moments of the electron beam as discussed in the next section.

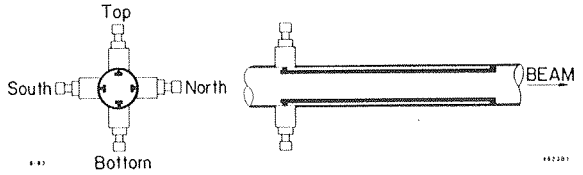

Fig. 1. Stripline position monitor.

Multipole Expansion of Image Current Density Given a delta function line current, I, at the point (r, ϕ), the image current density, J, on a conducting cylinder of radius a at the point (a, θ) (see Fig. 2) is given by[3]

$$J_{image}(r, \phi, a, \theta) = \frac{I(r, \phi)}{2\pi a} \frac{a^2 - r^2}{a^2 + r^2 - 2ar\cos(\theta - \phi)} .$$

Expanding in powers of r/a gives

$$\begin{aligned} J_{image}(r, \phi, a, \theta) &= \frac{I(r, \phi)}{2\pi a}\left[1 + \sum_{k=1}^{\infty} \left(\frac{r}{a}\right)^k \cos k(\theta - \phi)\right] \\ &= \frac{I(r, \phi)}{2\pi a}\left\{1 + 2\left[\frac{x}{a}\cos\theta + \frac{y}{a}\sin\theta\right]\right. \\ &\quad + 2\left[\frac{x^2 - y^2}{a^2}\cos 2\theta + 2\frac{xy}{a^2}\sin 2\theta\right] \\ &\quad + 2\left[\left(\frac{x^3}{a^3} - 3\frac{xy^2}{a^3}\right)\cos 3\theta - \left(\frac{y^3}{a^3} - 3\frac{yx^2}{a^3}\right)\sin 3\theta\right] \\ &\quad \left. + \text{higher order terms}\right\} \end{aligned}$$

The total image current density due to a Gaussian charge distribution is given by

$$\begin{aligned} J_{image}(a, \theta) = &\frac{I_{beam}}{4\pi^2 a\sigma_x\sigma_y} \int\int_{\substack{area \\ of\ pipe}} \\ &\times \left[1 + 2\sum_{k=1}^{\infty}\left(\frac{r}{a}\right)^k \cos k(\theta - \phi)\right] \\ &\times \exp\left[\frac{(x - \bar{x})^2}{2\sigma_y^2}\right]\exp\left[\frac{(y - \bar{y})^2}{2\sigma_y^2}\right] da \end{aligned}$$

where I_{beam} = total beam current, $(\bar{x}, \bar{y})$ is the beam centroid and σ_x, σ_y are the rms half widths in the x and y directions.

In the case where σ_x and σ_y are small compared to the pipe radius, the integration is well approximated by integration to ∞. For the present discussion, a detailed analysis including error functions is not essential. The integration to ∞ yields

*Work supported by the Department of Energy, contract DE-AC03-76SF00515.

$$J_{image}(a,\theta) \simeq \frac{I_{beam}}{2\pi a}\left\{1 + 2\left[\frac{\bar{x}}{a}\cos\theta + \frac{\bar{y}}{a}\sin\theta\right]\right.$$
$$+ 2\left[\left(\frac{\sigma_x^2 - \sigma_y^2}{a^2} + \frac{\bar{x}^2 - \bar{y}^2}{a^2}\right)\cos 2\theta + 2\frac{\bar{x}\,\bar{y}}{a^2}\sin 2\theta\right]$$
$$+ 2\left[3\left(\frac{\sigma_x^2 - \sigma_y^2}{a^2}\right) + \frac{\bar{x}^2 - \bar{y}^2}{a^2}\right]\left(\frac{\bar{x}}{a}\cos 3\theta + \frac{\bar{y}}{a}\sin 3\theta\right)$$
$$\left. + \text{higher order terms}\right\}$$

The image currents are sampled at four values of θ, namely $\theta = 0$, $\pi/2$, π, and $3\pi/2$. The signals on the four stripline probes have monopole, dipole, quadrupole and sextupole components as shown in Table 1.

Monitor Sensitivity In order to determine the sensitivity of the stripline monitors to the quadrupole moment, we measured the quadrupole component of the wall current as a function of transverse beam displacement. Specifically, we measured the signals from the four probes of a single stripline monitor as we steered the beam first in the horizontal and then in the vertical plane. A plot of the quadrupole component of the wall current as a function of the beam's transverse position is shown in Fig. 3. We have plotted $q+2d_y^2$ versus d_x and $q-2d_x^2$ versus dy where

$$d_x \equiv \frac{N-S}{N+S+T+B} = \frac{\bar{x}}{a}\left[1 + 3\frac{\sigma_x^2 - \sigma_y^2}{a^2} + \frac{\bar{x}^2 - \bar{y}^2}{a^2} + \text{terms to higher order}\right]$$

$$d_y \equiv \frac{T-B}{N+S+T+B} = \frac{\bar{y}}{a}\left[1 + 3\frac{\sigma_x^2 - \sigma_y^2}{a^2} - \frac{\bar{x}^2 - \bar{y}^2}{a^2} + \text{terms to higher order}\right]$$

$$q \equiv \frac{(N+S)-(T+B)}{N+S+T+B} = 2\left[\frac{\sigma_x^2 - \sigma_y^2}{a^2} + \frac{\bar{x}^2 - \bar{y}^2}{a^2} + \text{terms to higher order}\right].$$

The axes of the steering dipoles were rotated slightly with respect to the stripline probes, consequently, when we steered the beam horizontally, $\bar{y}$ changed slightly. Thus we plotted $q + 2d_y^2$ versus d_x, as $2d_y^2$ cancels the contribution to q due to vertical beam displacement. Similarly, we have plotted $q - 2d_x^2$ versus d_y.

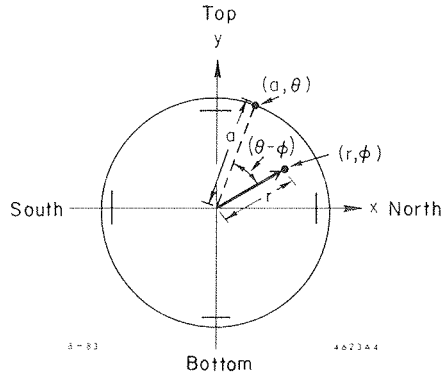

Fig. 2. Line current at (r, ϕ) inside conducting cylinder of radius a.

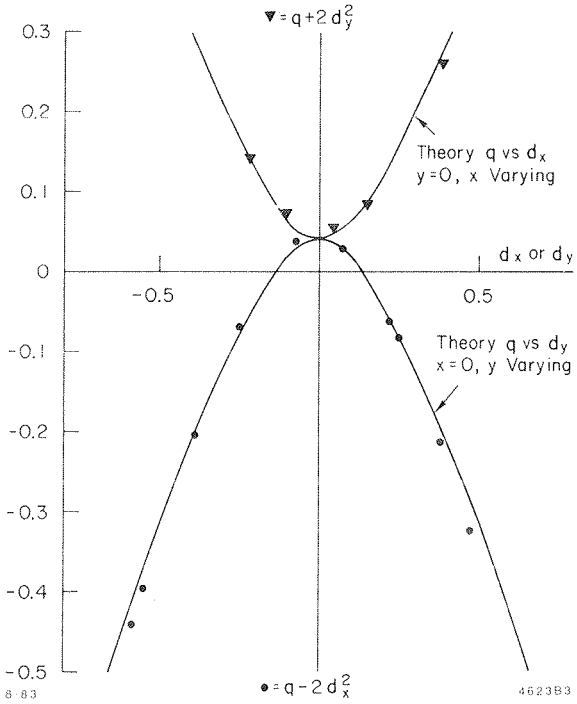

Fig. 3. Monitor Sensitivity. $q+2d_y^2$ versus d_x (triangles). $q-2d_x^2$ versus d_y (circles). Vertical intercept $= 2(\sigma_x^2 - \sigma_y^2/a^2)$.

It should be noted that the position signals, $d_x \simeq \bar{x}/a[1+(\bar{x}/a)^2]$ and $d_y \simeq \bar{y}/a[1+(\bar{y}/a)^2]$, are sensitive to the sextupole moment of the beam. For large values of $\bar{x}$ or $\bar{y}$ this is a significant effect and is included in the theoretical curves.

Table 1. Signal on Stripline Probes Normalized to $I_{beam}/2\pi a$

Strip	N = North ($\theta = 0$)	S = South ($\theta = \pi$)	T = Top ($\theta = \pi/2$)	B = Bottom ($\theta = 3\pi/2$)
Monopole	1	1	1	1
Dipole	$2\frac{\bar{x}}{a}$	$-2\frac{\bar{x}}{a}$	$2\frac{\bar{y}}{a}$	$-2\frac{\bar{y}}{a}$
Quadrupole	$2\left[\frac{\sigma_x^2-\sigma_y^2}{a^2} + \frac{\bar{x}^2-\bar{y}^2}{a^2}\right]$	$2\left[\frac{\sigma_x^2-\sigma_y^2}{a^2} + \frac{\bar{x}^2-\bar{y}^2}{a^2}\right]$	$-2\left[\frac{\sigma_x^2-\sigma_y^2}{a^2} + \frac{\bar{x}^2-\bar{y}^2}{a^2}\right]$	$-2\left[\frac{\sigma_x^2-\sigma_y^2}{a^2} + \frac{\bar{x}^2-\bar{y}^2}{a^2}\right]$
Sextupole	$2\frac{\bar{x}}{a}\left[3\frac{\sigma_x^2-\sigma_y^2}{a^2} + \frac{\bar{x}^2-\bar{y}^2}{a^2}\right]$	$-2\frac{\bar{x}}{a}\left[3\frac{\sigma_x^2-\sigma_y^2}{a^2} + \frac{\bar{x}^2-\bar{y}^2}{a^2}\right]$	$-2\frac{\bar{y}}{a}\left[3\frac{\sigma_x^2-\sigma_y^2}{a^2} + \frac{\bar{x}^2-\bar{y}^2}{a^2}\right]$	$2\frac{\bar{y}}{a}\left[3\frac{\sigma_x^2-\sigma_y^2}{a^2} + \frac{\bar{x}^2-\bar{y}^2}{a^2}\right]$

The measurements plotted in Fig. 3 confirm that the stripline monitors are adequately sensitive to the quadrupole component of the wall currents. In addition the measurements show that q varies quadratically with d_x and d_y as predicted by the theory. In the six monitors tested, the electrical center for the quadrupole moment coincided with the electrical center for the dipole moment to within 0.1 mm and the agreement with theory was as good as that in Fig. 3.

Emittance Fitting The quadrupole mode signal, q, from the stripline position monitors can be used to determine the parameters of the beam matrix. This may be accomplished because the beam sizes within the accelerator are simply related to the beam matrix at a specified reference point. In general one requires six independent measurements of the quadrupole moments to deduce the six parameters of the beam matrix, σ_{11}, σ_{12}, σ_{22}, σ_{33}, σ_{34}, and σ_{44}. These six measurements may be gathered from separate position monitors strategically placed in the linac, or from a pair of monitors separated by a quadrupole. The former geometry allows for a nondisruptive measurement of the beam thereby permitting pulse to pulse emittance monitoring. The latter method will necessarily interrupt operations while selected quadrupole magnet strengths are varied in order to generate the six measurements of quadrupole mode signals from the two monitors. Throughout the following discussion, TRANSPORT[4] notation will be used.

In the absence of $x-y$ coupling, the square of the beam size at a stripline monitor, σ_{11} and σ_{33} for the x and y planes, respectively, is related to the beam sigma matrix, σ^0_{ij}, at an upstream reference point via:

$$\sigma_{11} = (R_{11})^2\sigma^0_{11} + 2R_{11}R_{12}\sigma^0_{12} + (R_{12})^2\sigma^0_{22} \quad ,$$

and

$$\sigma_{33} = (R_{33})^2\sigma^0_{33} + 2R_{33}R_{34}\sigma^0_{34} + (R_{34})^2\sigma^0_{44} \quad ,$$

wherein the R_{ij} are the ij elements of the TRANSPORT matrix describing the machine lattice between the reference location and the particular stripline monitor. The quadrupole moment about the beam centroid is defined as $Q \equiv \sigma_x^2 - \sigma_y^2$. Q at the k^{th} monitor is given by

$$Q_k \equiv {}^k\sigma_{11} - {}^k\sigma_{33} = M_{ki}\sigma^0_i + \xi_k$$

for which summation over similar indices is implied, $\sigma^0_1 = \sigma^0_{11}$, $\sigma^0_2 = \sigma^0_{12}$, $\sigma^0_3 = \sigma^0_{22}$, $\sigma^0_4 = \sigma^0_{33}$, $\sigma^0_5 = \sigma^0_{34}$, and $\sigma^0_6 = \sigma^0_{44}$, and $M_{k1} = (R_{11})^2_k$, $M_{k2} = (2R_{11}R_{12})_k$, $M_{k3} = (R_{12})^2_k$, $M_{k4} = -(R_{33})^2_k$, $M_{k5} = -(2R_{33}R_{34})_k$, $M_{k6} = -(R_{34})^2_k$. The ξ_k are the errors in the measurements of the Q_k.

Given a sufficiently large set of Q_k's and M_{ki}'s (at least six rows are required), the beam matrix can be found using a weighted least squares fit:

$$[Q'] = [M'][\sigma^0]$$

yielding

$$[\sigma^0] = ([M]^t[M'])^{-1}[M]^t[Q']$$

with $M'_{ki} = \omega_k M_{ki}$, $Q'_k = \omega_k Q_k$, where ω_k = the weight factor of the quadrupole mode signal of the k^{th} monitor, and $[M]^t$ is the transpose of $[M]$.

From the calculated σ^0, the x and y plane emittances are given, respectively, as ϵ_x and ϵ_y:

$$\epsilon_x = (\sigma^0_1\sigma^0_3 - (\sigma^0_2)^2)^{1/2}$$

and

$$\epsilon_y = (\sigma^0_4\sigma^0_6 - (\sigma^0_5)^2)^{1/2}$$

The error in the determination of the emittances are taken to be the standard deviations of ϵ_x and ϵ_y. These are given by

$$\text{Error } (\epsilon_x) = \Big((\sigma^0_1)^2C_{33} + (\sigma^0_3)^2C_{11} - 4(\sigma^0_2)^2C_{22} - 2\sigma^0_1\sigma^0_3C_{13} - 2\sigma^0_1\sigma^0_2C_{23} - 2\sigma^0_2\sigma^0_3C_{12}\Big)^{\frac{1}{2}} \Big/ 2\epsilon_x$$

$$\text{Error } (\epsilon_y) = \Big((\sigma^0_4)^2C_{66} + (\sigma^0_6)^2C_{44} - 4(\sigma^0_5)^2C_{55} + 2\sigma^0_4\sigma^0_6C_{46} - 2\sigma^0_4\sigma^0_5C_{56} - 2\sigma^0_5\sigma^0_6C_{45}\Big)^{\frac{1}{2}} \Big/ 2\epsilon_y$$

in which the C_{ij} are the ij elements of the covariance matrix,

$$[C] = \left[\frac{([Q'] - [M'][\sigma^0])^t([Q] - [M][\sigma^0])}{N-6}([M]^t[M'])^{-1}\right]$$

wherein N is the number of Q measurements.

A simulation has been performed to test the foregoing method of emittance measurement. Figures 4a and 4b illustrate the geometry of the focusing lattice in the first sector of the SLAC linac along with the calculated beam sizes for a 72° phase shift/cell SLC trial lattice. The quadrupole moments of the beam in the existing stripline monitors (located inside the quadrupole focusing magnets) are displayed in Fig. 4c.

For these figures, a PEP gun beam emittance area of $\epsilon\gamma = 10^{-2}\pi$ m_0c-cm in each plane has been assumed and unSLEDded klystron gains have been used. A TRANSPORT calculation of this lattice was made, from which the quadrupole moments at the first six stripline monitors were tabulated, using the calculated beam sizes, along with the appropriate elements of the $[M]$ matrix. For the case of six Q_k's, a simple matrix inversion was performed on $[M]$ to determine the initial beam matrix. As was expected, the calculated beam matrix matched the input TRANSPORT beam card. It should be noted that an ideal FODO array set to 90° phase shift per cell is not suitable for this method of emittance measurement. This is a consequence of the fact that the beam is imaged every two FODO cells. Similarly, a distribution of stripline monitors within a drift section without intervening quadrupole lenses does not provide the necessary independence in the Q_k measurements.

An Emittance Measurement Table 2 shows the measured quadrupole mode of a single bunch CID beam in the first sector of the SLAC linac, recorded during an SLC linac test in June of 1983. Included in the table are the quadrupole magnet strengths, the beam energies at the various beam position monitors, as well as the estimated number of electrons in the bunch at the monitors. Transmission from the CID gun to the beginning of Sector I was estimated to be about 50%.

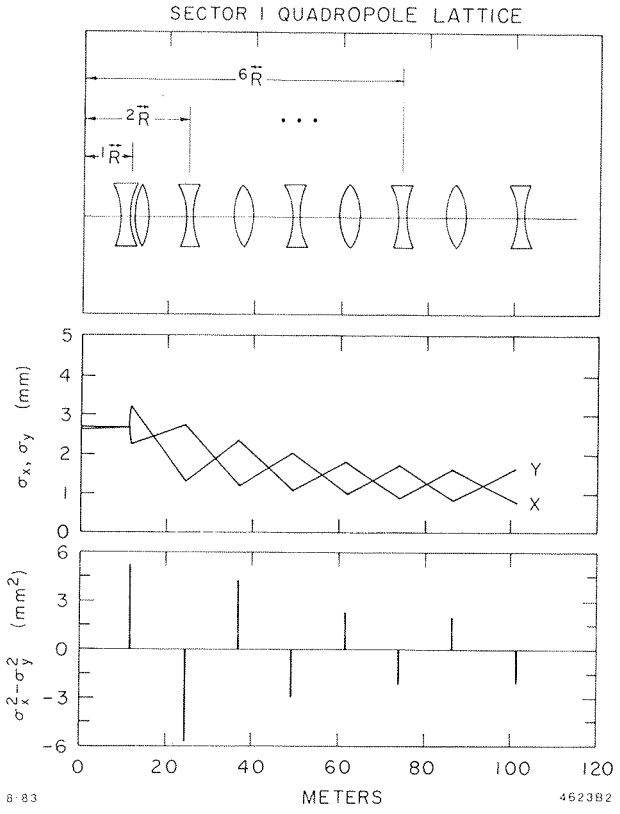

Fig. 4. (a) Quadrupole lattice in first 100 meters of the linac; (b) σ_x and σ_y versus z; (c) $\sigma_x^2 - \sigma_y^2$ versus z.

Table 2. Quadrupole Mode Data

Z-position (m)	Quadrupole Strength (kg)	Beam Energy (MeV)	Number of e^- ($\times 10^{10}$)	Q_k (cm^2)
0.0	–	85	3.5	–
11.5	−5.9	205	3.5	0.005
11.8	6.5	205	3.5	–
24.6	−1.0	322	2.7	−0.007
37.0	1.8	440	1.7	0.056
49.3	−2.3	551	1.2	−0.101
61.6	2.7	673	1.2	0.104
74.0	−3.2	790	1.2	−0.104
86.3	3.5	883	1.2	0.039
101.4	−4.0	995	1.2	−0.038

The lattice information (i.e., the quadrupole strengths and beam energies) was used in a TRANSPORT calculation to generate a 6×6 $[M]$ matrix for the last six monitors, for which the relative beam transmission is essentially flat; the sector entrance was taken to be the reference point. Data from these last six monitors along with $[M]$ was used to calculate a horizontal emittance area of $2.4 \times 10^{-2}\pi$ m_0c-cm and a vertical emittance area of $2.1 \times 10^{-2}\pi$ m_0c-cm. These numbers are consistent with measurements made using a different method,[5] at about $6 \times 10^{10} e^-$ per bunch. Given that this is a single data sample, statistical analysis is not possible. Further tests of the method and comparisons with intercepting emittance measurements are planned for the fall.

References

1. J.-L. Pellegrin, Proceedings of the 11^{th} International Conference on High Energy Accelerators, 459, 7-11 July 1980.
2. J. E. Clendenin *et al.*, Proceedings of the 1981 Linear Accelerator Conference, 130, 19-23 October 1981.
3. R. T. Avery *et al.*, IEEE Trans. Nucl. Sci. **NS-18**, 920, June 1971.
4. K. L Brown *et al.*, SLAC-91, Rev. 2 (1977).
5. J. C. Sheppard *et al.*, IEEE Trans. Nucl. Sci. **NS-30**, 2161, August 1983.